Shigella hijacks host ISGylation pathway by arginine ADP-riboxanation of HERC5

Xiaoyun Liu[1], Jie Jin[1], Xianbin Meng[2], Yi Yuan[1], Yi Huo[3], Jia Song[4], Xuliang Deng[4], and Haiteng Deng[2]

[1]Peking University School of Basic Medical Sciences
[2]Tsinghua University School of Life Sciences
[3]BeiGene (Beijing) Co Ltd
[4]Peking University School of Stomatology Department of General Dentistry

June 20, 2023

Abstract

Shigella flexneri type III effector OspC3 was recently found to evade host pyroptosis by targeting caspase-11 for ADP-riboxanation. The ADP-riboxanase activity was shared by its paralogues, OspC1 and OspC2, whereas the host substrates of them are still unknown. To solve this problem, we employed eAf1521 enrichment coupled with mass spectrometry (MS)-based proteomics to profile the host substrates of OspC1. In this study, we identified HERC5 as a host target of OspC1. As described previously, HERC5 functions as an E3 ISG15 ligase and catalyzes the ISGylation of a huge subset of host and pathogen proteins upon bacterial infection. Here, we show that *S. flexneri* hijacks host ISGylation pathway by OspC1-catalyzed ADP-riboxanation of HERC5 to promote its own survival and proliferation in host cells.

Introduction

Shigella flexneri is a gram-negative bacterial pathogen that causes communicable human bacillary dysentery (Trofa et al., 1999). During infection, *S. flexneri* manipulate various host processes by delivering effector proteins into host cells via its type III secretion system (T3SS) to promote development of its intracellular replicative niche and intercellular transmission (Mattock et al., 2017). Bacterial effectors are always found to be enzymes that often target host substrates for post-translational modifications (PTM) (Chambers et al., 2020). Among *S. flexneri* T3SS effectors, OspC family proteins, including OspC1, OspC2, and OspC3, have recently been demonstrated to possess ADP-riboxanase activity and catalyze ADP-riboxanation (541.06 Da), a derivative of ADP-ribosylation (524.03 Da) (Li et al., 2021). In the same study, human caspase-4 and mouse caspase-11 were identified to be the host targets of OspC3, which blocks the host pyroptosis-mediated defence. However, the host targets of its paralogues, OspC1 and OspC2, are still unknown and remain to be further investigated.

Accumulating evidence indicates that secreted bacterial nucleic acids could also be recognized by the traditionally believed cytosolic viral RNA and DNA sensors RIG-I, MDA5, and STING thereby triggering IFN-β production and anti-bacterial defence (Abdullah et al., 2012; Dobbs et al., 2015). To establish a vacuolar niche inside host cells, bacterial pathogens have evolved effectors to hijack these innate immune pathways. For instance, the *Coxiella burnetii* effector EmcB acts as a deubiquitinase and thwarts host RIG-I signaling by preferentially cleaving its K63-linked ubiquitin chains (Duncan-Lowey et al., 2023), whereas the *S. flexneri* effector IpaJ blocks STING translocation from endoplasmic reticulum (ER) to ER-Golgi intermediate compartments (ERGIC) thereby inhibiting its activation (Dobbs et al., 2015).

In the present study, we identified HERC5 as a host substrate of ADP-riboxanation catalyzed by *S. flexneri* effector OspC1 using a previously described strategy involving eAf1521 enrichment and mass spectrometry (MS)-based proteomics (Jin et al., 2023). HERC5 is highly inducible upon type I interferon stimulation and bacterial infection (Han et al., 2018), and functions as an E3 ISG15 ligase catalyzing the ISGylation of proteins (i.e., RIG-I, MDA5, and IRF3) implicated in innate immunity (Kim et al., 2008; Liu et al., 2021; Shi et al., 2010). Given that ISG15 and ISGylation themselves counteract *Listeriamonocytogenes* and mycobacteria infection via different mechanisms (Radoshevich et al., 2015; Swaim et al., 2017), we proposed that*S. flexneri* effector OspC1 may subvert host anti-bacterial defence by targeting HERC5 for ADP-riboxanation and thus inhibiting HERC5-catalyzed ISGylation. However, to our surprise, OspC1-catalyzed HERC5 ADP-riboxanation promotes its E3 ISG15 ligase activity and the overall ISGylation levels in the whole cell lysates slightly. To understand this confusing experimental result, we extensively reviewed the related literatures in detail, and found that not all ISGylation positively regulate host innate immune response. Indeed, HERC5-catalyzed ISGylation of MDA5 and IRF3 promote the host antiviral immunity (Liu et al., 2021; Shi et al., 2010), whereas HERC5-catalyzed RIG-I ISGylation induced by Type I interferon negatively regulates RIG-I-mediated antiviral signaling as a feedback mechanism (Kim et al., 2008). It is reasonable that HERC5 targets different proteins for ISGylaton to positively and negatively regulate the host immunity precisely and thus avoid excessive inflammatory damage. Inspired by this finding, we determined two documented HERC5-catalyzed ISGylation substrates (i.e., HERC5 itself and RIG-I) with ISG15-conjugating system in the presence of wild-type or catalytically mutated OspC1 (Wong et al., 2006; Kim et al., 2008; Zhao et al., 2005), and found that OspC1-mediated HERC5 ADP-riboxanation upregulates the ISGylation of HERC5 and RIG-I, resulting in the downregulation of host anti-*Shigella* defence.

Results

Identification of HERC5 as a host substrate of *S. flexneri* effector OspC1

To identify host substrates of *S. flexneri* effector OspC1, we overexpressed empty vector (EV) or wild-type (WT) OspC1 in 293T cells. ADP-riboxanated and ADP-ribosylated proteins were isolated with eAF1521-conjugated beads from EV or WT OspC1-transfacted cell lysates and then digested with trypsin and subjected to mass spectrometry (MS) analysis as described in our previous publication (Figure 1a; Jin et al., 2023). As we expected, ADP-riboxanation or ADP-ribosylation signals were significantly stronger, and more proteins were enriched in WT group than in EV group (Figure 1b, c). In the proteomic dataset, we noticed an extremely familiar protein HERC5, which we have studied before (Jin et al., 2021), was detected in the WT group other than the EV group (Supplementary Table 1). Known that ISG15-conjugating system including HERC5 are highly inducible upon type I interferon stimulation or bacterial infection, we tried to verify HERC5 as a host substrate of*S. flexneri* effector OspC1 in the overexpression system with WT OspC1 or its catalytic dead mutant (MUT) OspC1$^{E187A/H322A}$. Fortunately, we confirmed that HERC5 is indeed a host substrate of *S. flexneri* effector OspC1 (Figure 1d).

Identification of Arg44 and Arg663 in HERC5 as the major ADP-riboxanation sites

To determine the ADP-riboxanation sites in HERC5 catalyzed by *S. flexneri* effector OspC1, we perfomed LC-MS/MS analysis. Briefly, HERC5-Flag with WT or MUT OspC1 were co-overexpressed in 293T cells and HERC5-Flag proteins were immunoprecipitated with anti-Flag agarose and then separated by SDS-PAGE (Figure 1e). The target band corresponding to HERC5-Flag were harvested and subjected to in-gel digestion with trypsin, followed by LC-MS/MS analysis in collision-induced dissociation (CID) mode. Our analysis indicated that HERC5 was ADP-riboxanated at Arg44 and Arg663 sites by *S. flexneri* effector OspC1 (Figure 2a, b; Supplementary Figure 1).

The presence of diagnostic ions with *m/z* of 136.06, 250.09, 348.05 and 428.04 which are adenine$^+$, adenosine - H_2O^+, adenosine monophosphate$^+$ (AMP^+), adenosine diphosphate$^+$ (ADP^+) in MS/MS spectra allowed the detection of putative ADP-riboxanated peptides (Li et al., 2021; Peng et al., 2022). However, due to the mass discrimination in CID mode, we only detected the diagnostic marker ions at *m/z* 348.07 (AMP^+) and 428.04 (ADP^+) (Figure 2a). We re-performed the LC-MS/MS analysis in high energy collision dissociation

(HCD) mode, and fortunately detected all of the diagnostic ions mentioned above (Figure 2b; Supplementary Figure 1). By quantitative analysis, we determined that about 45% of total HERC5 were ADP-riboxanated at Arg44 by *S. flexneri* effector OspC1 (Figure 2c).

HERC5 was also ADP-ribosylated by *S. flexneri* effector OspC1 at Arg44

As reported, ADP-riboxanation (524.03 Da) involves an additional deamidation upon the conventional ADP-ribosylation (541.06 Da) (Figure 3c; Li et al., 2021; Peng et al., 2022). Indeed, ADP-ribosylated peptide was detected in our MS/MS data, which indicated that *S. flexneri*effector OspC1 could also ADP-ribosylated HERC5 at Arg44 (Figure 3a). Quantitative analysis suggested that the ratio of ADP-ribosylation and ADP-riboxanation of HERC5 at Arg44 was about 1:10 (Figure 3b). The same phenomenon was also observed by previous investigators, but the ratio they observed is much lower (1:1000) (Peng et al., 2022). In that study, the trace amount of ADP-ribosylated caspase-3 at Arg207 was interpreted as the intermediate of ADP-riboxanated caspase-3 catalyzed by*Chromobacterium violaceum* CopC (Peng et al., 2022). However, based on our result, we tend to believe that the additional deamidation is reversible and the ADP-ribosylated HERC5 at Arg44 is the product of the reversible reaction from ADP-riboxanated HERC5 (Figure 3c). Unfortunately, there is still no further experimental evidence to support our hypothesis.

ADP-riboxanation upregulates the E3 ISG15 ligase activity of HERC5

To determine the biological function of HERC5 ADP-riboxanation catalyzed by *S. flexneri* effector OspC1, we overexpressed the ISG15-congjugating system together with WT or MUT OspC1 in 293T cells. As reviewed in the previous publication and observed in our experiment, only free ISG15, but not ISGylation, was induced upon type I IFN stimulation (Zhang et al., 2011; Figure 4a). That being said, the ISGylation observed in the overexpression experiments were all caused by exogenous expression of ISG15-congjugating system (Figure 4b). Comparing to the MUT group, the ISGylation generated in the WT group were much stronger (Figure 4c), which indicated that ADP-riboxanation of HERC5 catalyzed by *S. flexneri* effector OspC1 promoted the activity of its E3 ISG15 activity.

To further verify this conclusion, we tested the ISGylation of HERC5 itself and RIG-I in the overexpression system in the presence of WT or MUT OspC1, and found that the ISGylation of HERC5 itself was enhanced slightly, whereas the ISGylation of RIG-I was promoted by *S. flexneri* effector OspC1 significantly. Given that the ISGylation of RIG-I negatively regulates its activation as a feedback mechanism to fine-tune host innate immune response (Kim et al., 2008),*Shigella* may subvert host innate anti-bacterial defence by hijacking this negative mechanism via OspC1-catalyzed HERC5 ADP-riboxanation, which results in the accumulation of non-functional ISGylated RIG-I in the host cells.

Discussion

In this study, we identified HERC5 as a host substrate of ADP-riboxanation catalyzed by *S. flexneri* effector OspC1, which promoted its E3 ISG15 ligase activity. Considering that HERC5 itself showed quite strong enzymatic activity in the overexpression system (Figure 4b), it was not surprising to observe that the ISGylation was subtly enhanced by ADP-riboxanated HERC5, comparing to unmodified HERC5 (Figure 4c). Besides, ADP-riboxanated HERC5 specifically upregulates the ISGylation of certain substrates with varying degrees (Figure 4d-e), so that the global change of ISGylation on the whole cell level were neutralized by those unchanged or changed slightly.

In addition to ADP-riboxanated peptide, ADP-ribosylated peptide of HERC5 was also detected in our LC-MS/MS analysis (Figure 3a). Coincidentally, ADP-ribosylated peptide of caspase-3 had also been detected when studying ADP-riboxanation (also designated as ADPR-deacylization) of caspasa-3 catalyzed by *C. violaceum* CopC (Peng et al., 2022). The trace amount of ADP-ribosylated peptide of caspase-3 detected led them to interpret it as the intermediate of ADP-riboxanated caspase-3. However, the stoichiometric ratio of ADP-ribosylated HERC5 to ADP-riboxanated HERC5 observed in our system was 100 times higher than that of ADP-ribosylated caspase-3 to ADP-riboxanated caspase-3 (Figure 3b). Despite no additional experimental evidence currently, we tend to believe ADP-ribosylated HERC5 is the reversible product of

ADP-riboxanated HERC5 (Figure 3c).

Traditionally, cytosolic nucleic acid sensors such as RIG-I, MDA5, and STING, and downstream transcription factor IRF3 were believed to only respond to viral RNA or DNA. However, a growing body of studies suggests that they also sense bacterial DNA and RNA and induce innate immune response defensing against bacterial infection by promoting the expression of type I interferons. Upon bacterial infection and type I interferon stimulation, the ISG15-conjugating system are also highly induced to modify a huge subset of host substrates, especially those participating anti-bacterial defence, by ISGylation. As mentioned above, RIG-I and STING activation were blocked by the *C. burnetii*effector EmcB and *S. flexneri* effector IpaJ respectively (Duncan-Lowey et al., 2023; Dobbs et al., 2015), indicating that RIG-I and STING signaling play indispensable roles in anti-bacterial defence. Additionally, bacteria also evolved strategies to counteract host ISG15- and ISGylation-mediated anti-bacterial defence (Radoshevich et al., 2015; Swaim et al., 2017). As shown in Figure 5, we found that *S. flexneri* effector OspC1 could target host E3 ISG15 ligase HERC5 for ADP-riboxanation and then specifically upregulate the ISGylation of RIG-I, thereby inhibiting its activation. It provided novel insights into the roles of ADP-riboxanation employed by *S. flexneri*to manipulate host anti-bacterial defence.

Experimental Procedures

Cell culture and transfection

293T cells were cultured in DMEM (Gibco, 11965092) supplemented with 10% FBS (TransSerum, FS101-02) at 37 incubator with 5% CO_2. 293T cells were kept in our laboratory. Polyethylenimine (PEI) (Sigma-Aldrich, 9002-98-6) were used to transiently transfect DNA constructs into 293T cells.

Co-Immunoprecipitation and Western Blot assays

Cells were harvested from 10 cm dishes 24 h after transfection and lysed with 500 μl lysis buffer (150 mM NaCl, 20 mM Tris-HCl (pH=7.5), 1% Triton X-100, 1% sodium deoxycholate, 1× PMSF, and sodium fluoride). Suspended cell lysates (400 μl) was taken to incubate with anti-Flag M1 agarose affinity gel (Sigma-Aldrich, A4596-5ml) for 4 h or overnight at 4 . The immunoprecipitates were washed five times with 1 ml lysis buffer for 5 min each and then boiled at 98 for 10 min in 65 μl 2× sample loading buffer. The rest cell lysates (100 μl) were diluted with 5× sample loading buffer and boiled at 98 for 10 min, followed by western blot analysis.

The samples were subjected to SDS-PAGE and then transferred to 0.45 μm Polyvinylidene fluoride (PVDF) membrane (Merck millipore, IPVH00010). PVDF membranes were blocked in 5% non-fat milk prepared with Tris-buffered salined with Tween 20 (TBST) for 1 h, and incubated with corresponding primary antibody, second HRP-linked IgG at room temperature in 5% non-fat milk for 2 h each successively. After each incubation, PVDF membranes were washed five times with TBST for 5 min each. Target proteins were detected with ECL reagent (Tanon, XSK-180-5001) and photographed by chemiluminescence imager (Tanon, 5200).

LC-MS/MS analysis

HERC5-Flag, along with WT or MUT OspC1, overexpressed in 293T cells was immunoprecipitated with anti-Flag M1 agarose affinity gel (Sigma-Aldrich, A4596-5ml) 24 h after transfection and then subjected to SDS-PAGE separation and Coomassie Blue staining. Target HERC5-Flag bands were taken for in-gel digestion with trypsin according to a standard protocol, followed by Liquid chromatography-tandem mass spectrometry (LC-MS/MS) analysis on Thermo Scientific^{TM} Orbitrap Fusion^{TM} coupled with UltiMate3000. The MS/MS spectra of modified peptides were acquired by searching the raw data with Mascot (version 2.3.02, Matrix Science).

Antibody and reagents

Rabbit anti-Poly/Mono-ADP-ribose (E6F6A) (CST, 83732S) (1:1000), rabbit anti-Flag (ZENBIO, R24091) (1:2000), mouse anti-Flag (ZENBIO, 250111) (1:2000), Rabbit anti-HA (ZENBIO, 390001) (1:2000), Mouse

anti-Myc (ZENBIO, 250112) (1:2000), Mouse anti-GFP (EASYBIO, BE2001-100UL) (1:2000), Mouse anti-β -actin (CST, 4970S) (1:2000), Mouse anti-ISG15 (Santa Cruz, sc-166755), HRP-linked horse anti-mouse IgG (CST, 7076S) (1:2000), HRP-linked goat anti-rabbit IgG (CST,7074S)(1:2000), IFN-β (Sino Biological, 10704-HNAS) were purchased from the corresponding manufactures.

DNA constructs

pLVX-EGFP-OspC1, pLVX-EGFP-OspC1(E187A/H322A), pEGFP-N1-UBE1L-Myc, pEGFP-N1-UBCH8-Myc, pCDNA3.1-HERC5-Myc, pCDNA3.1-HERC5-Flag, pCMV-HA-ISG15, pLVX-Flag-ISG15-IRES-ZsGreen1, pCDNA3.1-Flag-RIG-I.

Acknowledgements

We thank Liu lab members for discussion. We thank Prof. Haiteng Deng and Dr. Xianbin Meng in Protein Chemistry and Proteomics Facility at Technology Center for Protein Sciences, Tsinghua University, for assistance in protein MS analysis. The work was financially supported by grants from National Key Research and Development Program of China (2022YFA1304500), the Natural Science Foundation of China (22174003 and 21974002), Peking University Medicine Seed Fund for Interdisciplinary Research and the Fundamental Research Funds for the Central Universities.

ORCID

Jie Jin https://orcid.org/0000-0001-8641-8843

Xiaoyun Liu https://orcid.org/0000-0001-7083-5263

Author contributions

Jie Jin designed the study and performed almost all the experiments except those contributed by others listed below. Jie Jin analyzed the data, prepared the figures, and wrote the original draft. Xianbin Meng assisted in the LC-MS/MS analysis. Yi Yuan provided assistance in the daily experiments such as protein purification and molecular cloning. Haiteng Deng and Yi Huo contributed the plasmid encoding ISG15 conjugating system including ISG15, UBE1L, UBCH8, and HERC5. Xuliang Deng and Jia Song contributed the plasmid encoding RIG-I. Xiaoyun Liu supervised the study, obtained the funding, and rewrote the manuscript.

Data availability statement

The data that support the findings of this study are available from the corresponding author upon reasonable request.

Ethics statement

This study was approved by the ethical review board of School of Basic Medical Sciences, Peking University Health Science Center. There were no animal models or human subjects involved in this study.

Conflict of interest

The authors declare no conflict of interest.

References

Abdullah, Z., Schlee, M., Roth, S., Mraheil, M.A., Barchet, W., Böttcher, J., et al. (2012) RIG-I detects infection with live*Listeria* by sensing secreted bacterial nucleic acids. *The EMBO Journal, 31,* 4153-4164.*https://doi.org/10.1038/emboj.2012.274.*

Chambers, K.A. & Scheck, R.A. (2020) Bacterial virulence mediated by orthogonal post-translational modification. *Nature Chemical Biology, 16,* 1043-1051.*https://doi.org/10.1038/s41589-020-0638-2.*

Dobbs, N., Burnaevskiy, N., Chen, D., Gonugunta, V.K., Alto, N.M. & Yan, N. (2015) STING activation by translocation from the ER is associated with infection and autoinflammatory disease. *Cell Host & Microbe, 18,* 157-168.*https://doi.org/10.1016/j.chom.2015.07.001.*

Duncan-Lowey, J., Crabill, E., Jarret, A., Reed, S.C.O. & Roy, C.R. (2023) The *Coxiella burnetii* effector EmcB is a deubiquitinase that inhibits RIG-I signaling. *Proceedings of the National Academy of Sciences of the United States of America, 120,* e2217602120.*https://doi.org/10.1073/pnas.2217602120*.

Han, H.G., Moon, H.W. & Jeon, Y.J. (2018) ISG15 in cancer: beyond ubiquitin-like protein. *Cancer Letters, 438,* 52-62.*https://doi.org/10.1016/j.canlet.2018.09.007*.

Jin, J., Meng, X., Huo, Y. & Deng, H. (2021) Induced TRIM21 ISGylation by IFN-β enhances p62 ubiquitination to prevent its autophagosome targeting. *Cell Death & Disease, 12,* 697.*https://doi.org/10.1038/s41419-021-03989-x*.

Jin, J., Yuan, Y., Xian, W., Tang, Z., Fu, J. & Liu, X. (2023) The ever-increasing necessity of mass spectrometry in dissecting protein post-translational modifications catalyzed by bacterial effectors.*Molecular Microbiology, 119,* 677-686.*https://doi.org/10.1111/mmi.15071*.

Kim, M.-J., Hwang, S.-Y., Imaizumi, T. & Yoo, J.-Y. (2008) Negative feedback regulation of RIG-I-mediated antiviral signaling by interferon-induced ISG15 conjugation. *Journal of Virology, 82,*1474-1483.*https://doi.org/10.1128/JVI.01650-07*.

Li, Z., Liu, W., Fu, J., Cheng, S., Xu, Y., Wang, Z. et al. (2021)*Shigella* evades pyroptosis by arginine ADP-riboxanation of caspase-11. *Nature, 599,* 290-295.*https://doi.org/10.1038/s41586-021-04020-1*.

Liu, G.Q., Lee, J.-H., Parker, Z.M., Acharya, D., Chiang, J.J., van Gent, M. et al. (2021) ISG15-dependent activation of the sensor MDA5 is antagonized by the SARS-CoV-2 papain-like protease to evade host innate immunity. *Nature Microbiology, 6,* 467-478.*https://doi.org/10.1038/s41564-021-00884-1*.

Mattock, E., & Blocker, A.J. (2017) How do the virulence factors of*Shigella* work together to cause disease? *Frontiers in Cellular and Infection Microbiology,* **7**, 64.*https://doi.org/10.3389/fcimb.2017.00064*.

Peng, T., Tao, X., Xia, Z., Hu, S., Xue, J., Zhu, Q. et al. (2022) Pathogen hijacks programmed cell death signaling by arginine ADPR-deacylization of caspases. *Molecular Cell, 82,* 1806-1820.e8.*https://doi.org/10.1016/j.molcel.2022.03.010*.

Radoshevich, L., Impens, F., Ribet, D., Quereda, J.J., Tham, T.N., Nahori, M.-A. et al. (2015) ISG15 counteracts *Listeriamonocytogenes* infection. *Elife, 4,* e06848.*https://doi.org/10.7554/eLife.06848*.

Shi, H.-X., Yang, K., Liu, X., Liu, X.-Y., Wei, B., Shan, Y.-F. et al. (2010) Positive regulation of interferon regulatory factor 3 activation by Herc5 via ISG15 modification. *Molecullar and Cellular Biology, 30,* 2424-2436.*https://doi.org/10.1128/MCB.01466-09*.

Swaim, C.D., Scott, A.F., Canadeo, L.A. & Huibregtse, J.M. (2017) Extracellular ISG15 signals cytokine secretion through the LFA-1 integrin receptor. *Molecular Cell, 68,* 581-590.e5.*https://doi.org/10.1016/j.molcel.2017.10.003*.

Trofa, A.F., Ueno-Olsen, H., Oiwa, R. & Yoshikawa, M. (1999) Dr. Kiyoshi Shiga: discoverer of the dysentery bacillus. *Clinical Infectious Diseases, 29,* 1303-1306.*https://doi.org/10.1086/313437*.

Wong, J.J., Pung, Y.F., Sze, N.S. & Chin, K.C. (2006) HERC5 is an IFN-induced HECT-type E3 protein ligase that mediates type I IFN-induced ISGylation of protein targets. *Proceedings of the National Academy of Sciences of the United States of America, 103,* 10735-10740.*https://doi.org/10.1073/pnas.0600397103*.

Zhang, D. & Zhang, D.-E. (2011) Interferon-stimulated gene 15 and the protein ISGylation system. *Journal of Interferon & Cytokine Reseach, 31,* 119-130.*https://doi.org/10.1089/jir.2010.0110*.

Zhao, C., Denison, C., Huibregtse, J.M., Gygi, S. & Krug, R.M. (2005) Human ISG15 conjugation targets both IFN-induced and constitutively expressed proteins functioning in diverse cellular pathways.*Proceedings of the National Academy of Sciences of the United States of America, 102,* 10200-10205.*https://doi.org/10.1073/pnas.0504754102*.

FIGURE 1 a Workflow used in our study to enrich and profile ADP-ribosylated and ADP-riboxanated proteins, which is adapted from our previous publication (Jin et al., 2023). **b-c** OspC1 from*S. flexneri* were expressed in 293T cells, and ADP-ribosylated or ADP-riboxanated proteins were isolated from cell lysates using eAf1521-conjugated beads. The samples and cell lysates were separated by SDS-PAGE, and then subjected to immunoblotting (b), or coomassie blue staining and LC-MS/MS analysis (c), respectively. **d** HERC5-Flag was co-expressed with wild-type (WT) OspC1 or catalytically dead mutant (MUT) OspC1 $^{E187A/H322A}$ in 293T cells. Cells were collected and lysed and subjected to immunoblotting with indicated antibodies, or immunoprecipitation with Flag antibodies, followed by immunoblotting with indicated antibodies. **e** HERC5-Flag isolated from WT or MUT OspC1-overexoressing 293T cell lysates were separated by SDS-PAGE and then subjected to coomassie blue staining.

FIGURE 2 a-b LC-MS/MS analysis of ADP-riboxanated HERC5-Flag in collision-induced dissociation (CID) mode (b) or in high energy collision dissociation (HCD) mode. Tandem mass (MS/MS) spectrums indicated that HERC5 was ADP-roboxanated at Arg44 and matched the fragmentation pattern of the modified peptide with many ADP-riboxanation-specific diagnostic ions and neutral loss fragments.**c** Extracted ion chromatograms of the reference peptide, unmodified peptide, and modified peptide with peak intensities.

FIGURE 3 a MS/MS spectrum matching the ADP-ribosylated peptide of HERC5 with ADP-ribosylation-specific diagnostic ions. **b**Extracted ion chromatograms of the ADP-ribosylated or ADP-riboxanated peptide. **c** Schematic illustration of the reaction of ADP-ribosylation and ADP-riboxanation adjusted from our previous publication (Jin et al., 2023).

FIGURE 4 a 293T cells were treated with IFN-β for indicated times and then harvested and lysed, followed by immunoblotting with indicated antibodies. **b** ISG15-conjugating system including Ube1L (E1), UBCH8 (E2), ISG15 were co-expressed with HERC5 (E3) or HERC5 and USP18 in 293T cells. Cells were collected and lysed for immunoblotting with indicated antibodies. **c** 293T cells overexpressing ISG15-conjugating system with WT or MUT OspC1 were harvested and lysed for immunoblotting with indicated antibodies.**d-e** Flag-tagged HERC5 (d) or RIG-I (e) were overexpressed with ISG15-conjugating system in the presence of WT or MUT OspC1 and isolated with anti-Flag agarose and then immunoblotted with anti-ISG15 antibody.

FIGURE 5 A working model for regulation of RIG-I signaling by*Shigella flexneri* effector OspC1-catalyzed HERC5 ADP-riboxanation. ADP-riboxanation of HERC5 promotes its E3 ISG15 ligase activity and then enhances the ISGylation of RIG-I, which results in the decrease of unmodified and functional RIG-I and thereby downregulation of RIG-I-mediated anti-bacterial defence.

FIGURE S1 Tandem mass (MS/MS) spectrums indicated that HERC5 was ADP-roboxanated at Arg663 and matched the fragmentation pattern of the modified peptide with ADP-riboxanation-specific diagnostic ions.

Figure 1

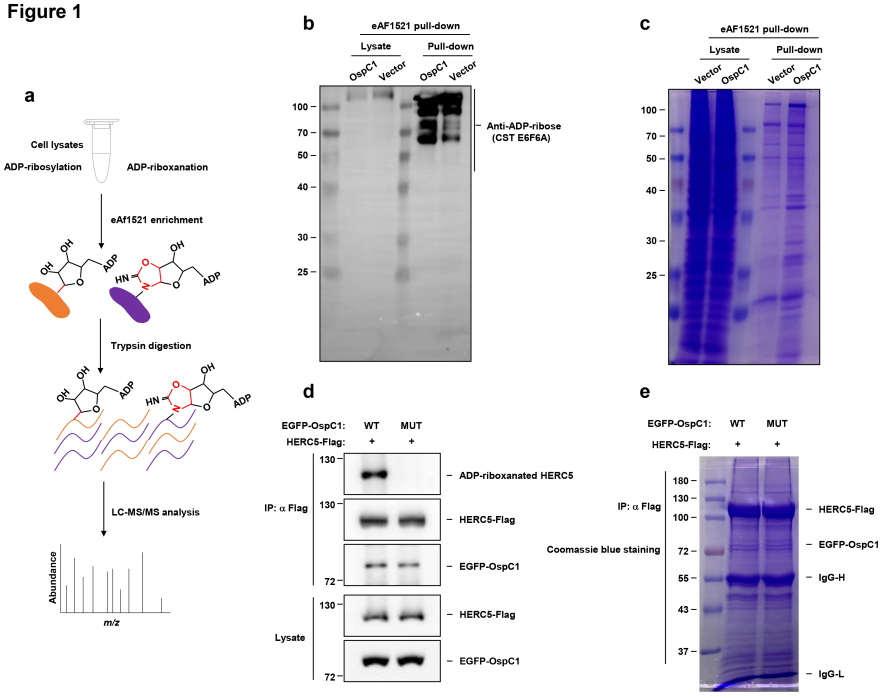

Figure 2

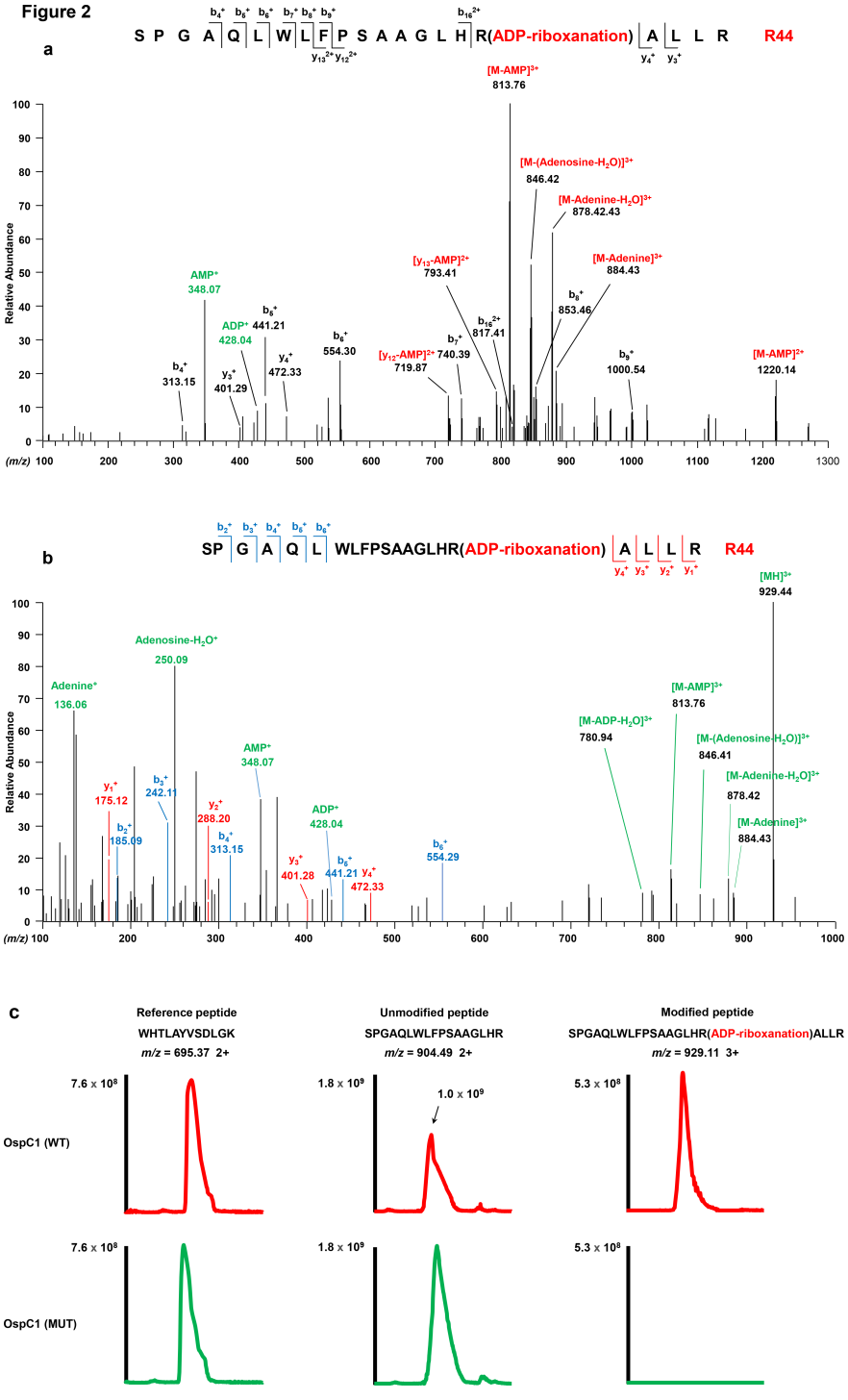

Figure 3

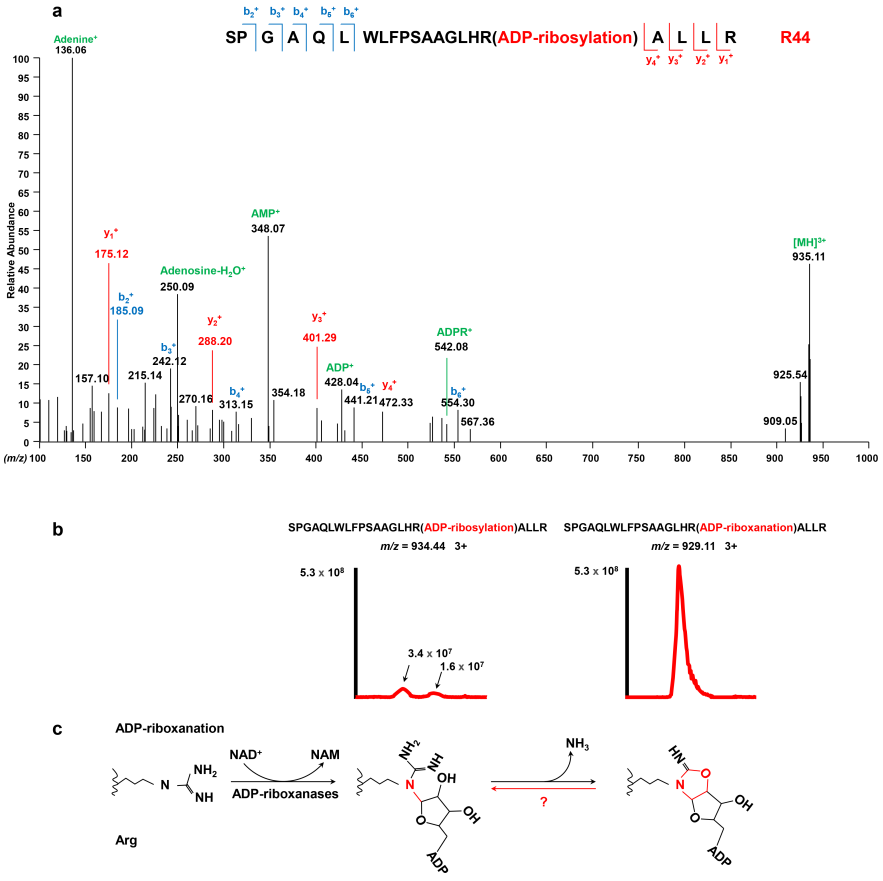

Figure 4

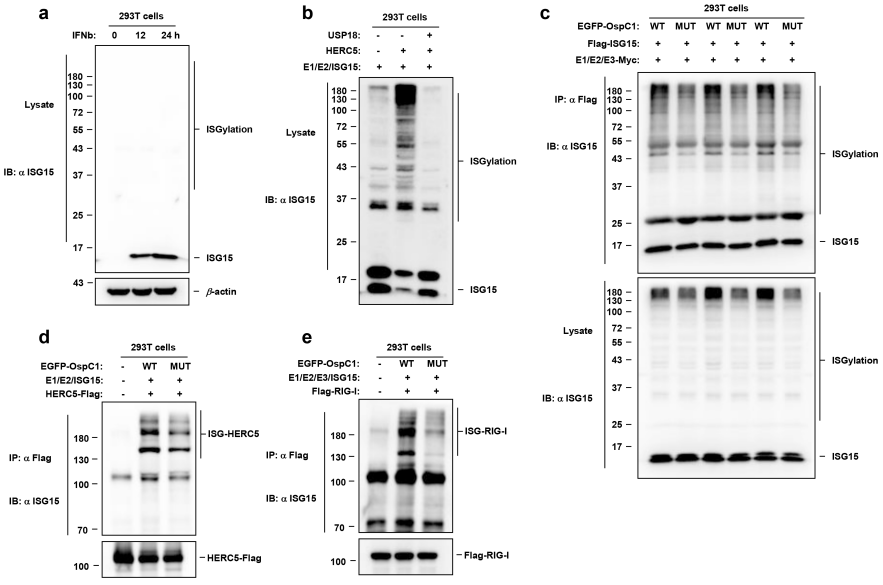

Figure 5

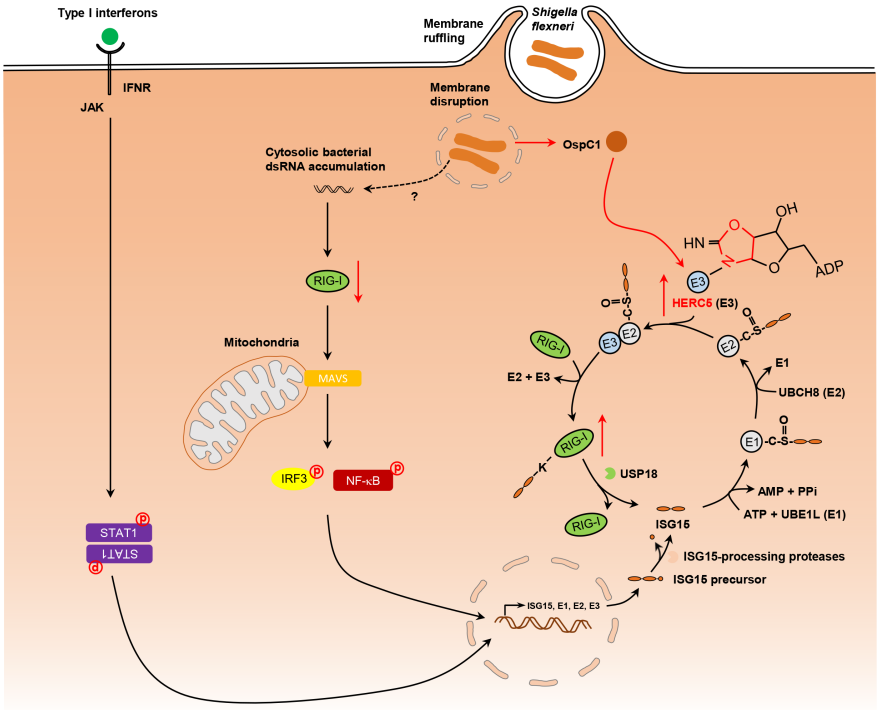

Figure S1